Pol. J. Environ. Stud. Vol. 34, No. 6 (2025), 8097-8114
DOI: *10.15244/pjoes/194585* ONLINE PUBLICATION DATE: 2025-03-05

Original Research

Research on the Evaluation and Prediction of the Prefabricated Cabin Substations Carbon Footprint Based on Life Cycle Theory and an Extreme Learning Machine

Ming Fang[1], Handong Lu[1], Xintian Fan[1], Shaohua Shi[2], Junjian Zhang[2]*

[1]Guangzhou Power Supply Bureau of Guangdong Grid Co, GuangZhou 510600, China
[2]Central Southern China Electric Power Design Institute Co., Ltd. of China Power Engineering Consulting Group, Wuhan 430064, China

Received: 19 August 2024
Accepted: 13 October 2024

Abstract

Prefabricated cabin substations, as a new type of substation, have advantages such as saving investment, a short construction period, and low-carbon environmental protection. They are the mainstream development trend of low-carbon substations in the future and play an important role in the construction of new power systems, especially in the development of urban power grids. This article systematically conducted carbon footprint tracing, analysis, calculation, and evaluation of prefabricated substations during the planning, construction, operation, and scrapping stages, forming a carbon footprint accounting method for the entire life cycle of prefabricated substations. The research results show that the carbon footprint of the construction and operation stages accounts for more than 90% of the carbon footprint of a prefabricated substation throughout its life cycle. Material carbon footprint, SF_6 carbon footprint, and station electricity carbon footprint are important components of the substation's carbon footprint. Green plants and lawns can effectively reduce the carbon emissions of prefabricated substations and have a positive effect on controlling carbon footprints. Suggestions were put forward to reduce the carbon footprint of prefabricated cabin substations in the areas of equipment replacement, energy conservation and consumption reduction, operation monitoring, and optimization. Simultaneously, carbon footprint prediction models for substations based on the bat algorithm (BA) and extreme learning machine (ELM) were constructed to accurately predict the carbon footprint of substations at various stages, providing a reference for the design selection, scheme optimization, energy-saving, and carbon reduction transformation of prefabricated cabin substations.

Keywords: carbon footprint, prefabricated cabin substation, full lifecycle, gray relational analysis, bat algorithm

*e-mail: 786214332@qq.com

Introduction

In recent years, the increase in greenhouse gases has led to global warming and frequent extreme weather events, which have adversely affected human production and life [1–3]. To effectively address climate change, China established a national carbon emissions trading market in July 2021 and took the lead in conducting carbon emissions trading in the power industry. As of now, China's carbon market has become the world's largest carbon market, covering greenhouse gas emissions. Prefabricated substations, as an important component of the power system, actively participating in carbon market trading is of great significance in reducing carbon emissions from prefabricated substations. Conducting a carbon footprint assessment of prefabricated substations can explore their carbon reduction potential and promote the green development of power grid enterprises [4–9].

With the accelerated construction of prefabricated substations, studying the full lifecycle carbon footprint of prefabricated substations is of great significance for controlling carbon emissions in the power industry and promoting the vigorous development of the carbon market in the power industry. According to the Second Biennial Update Report on Climate Change in China, China's greenhouse gas inventory includes six categories: carbon dioxide (CO_2), methane (CH_4), nitrous oxide (N_2O), hydrofluorocarbons (HFCs), perfluorides (PFCs), and sulfur hexafluoride (SF_6). The full lifecycle carbon footprint of prefabricated substations mainly includes the carbon footprint of greenhouse gases such as CO_2 and SF_6. This article focuses on studying the carbon footprint of prefabricated cabin substations throughout their entire lifecycle, starting from these two types of greenhouse gases (Fig. 1).

Many scholars at home and abroad have conducted research on the carbon footprints of substations. Liu et al. used the life cycle assessment method to calculate the carbon footprint of a 500 kV substation [10]. Zhao et al. studied the cost and carbon emission optimization calculation model for substations [11]. Liu et al. calculated the average carbon emissions of several West-East power transmission projects through Monte Carlo simulation [12]. Aryai et al. studied the differences in carbon emissions of power grids in different cities through electricity flow data [13]. Chen et al. proposed a comprehensive lifecycle cost for power transmission and transformation projects, including economic and carbon costs, and calculated these based on carbon market trading prices [14]. Lian et al. used the Granger causality test to verify the relationship between regional electricity carbon emissions and other factors [15].

Wei et al. studied the energy cost and related carbon footprint of ultra-high voltage substations in China [16]. Daneshzand et al. explored the impact of electric vehicle development on electricity prices and carbon emissions in response to the problem of potential power grid overload caused by electric vehicles [17]. Wang et al. studied the impact on the power grid as the penetration rate of renewable energy increases and proposed how to improve the carbon reduction capacity of the power grid through design optimization [18]. Desideri et al. evaluated the carbon emissions generated by the installation and transportation of photovoltaic system booster stations, taking into account the impact of global warming potential (GWP) [19]. Singh et al. calculated the carbon emissions changes of substations under different power factor operations [20]. Ruiz-Mendoza et al. defined the greenhouse gas emissions per unit of energy in electricity production as the carbon index and studied the relationship between the carbon index and power generation energy consumption in four Latin American countries [21]. Shaffer et al. proposed that deploying fuel cell clusters on the grid side can increase the penetration rate of renewable energy and continuously reduce carbon emissions [22].

Current research on the carbon footprint of substations mainly focuses on the carbon emissions of substations during the construction and operation phases. More in-depth research is still needed in many aspects: (1) A carbon footprint is the sum of greenhouse gas emissions and greenhouse gas removal, and current research is mainly limited to carbon emissions without studying carbon removal (i.e., negative emissions); (2) The study of carbon footprints in substations has overlooked the impact of GWP on research results. Taking SF_6 gas, a common gas in power distribution equipment, as an example, its greenhouse effect is 23900 times that of carbon dioxide; (3) Prefabricated cabin substations, as a new type of substation, have been widely used due to their low construction investment, short construction period, and convenient operation and maintenance. Currently, research on the carbon footprint of substations mainly focuses on traditional civil engineering substations, with less research on prefabricated cabin substations; (4) Lack of evaluation and calculation methods for the carbon footprint system of the entire life cycle cost of substations has prevented effective prediction of the carbon footprint of substations [23–28].

Based on the analysis of the current research status of carbon footprint in substations, this paper conducted a study on the evaluation and prediction of the carbon footprint of prefabricated cabin substations throughout their entire life cycle. The main innovations are as follows:

(1) The carbon footprint of prefabricated cabin substations is calculated in four stages: planning stage, construction stage, operation stage, and scrapping stage, covering the entire process of substation investment decision-making, construction, operation, and scrapping;

(2) Introducing Global Warming Potential (GWP) to convert the carbon footprint of substations into carbon dioxide equivalent, making the carbon footprint of each stage comparable, is of great significance for analyzing the carbon emission levels of prefabricated substations at different stages;

(3) We comprehensively calculated the carbon emissions and removal of substations and, for the first time, measured the carbon removal of substations represented by green plants and lawns in substations, providing reliable support for the scientific evaluation of substations carbon footprint;

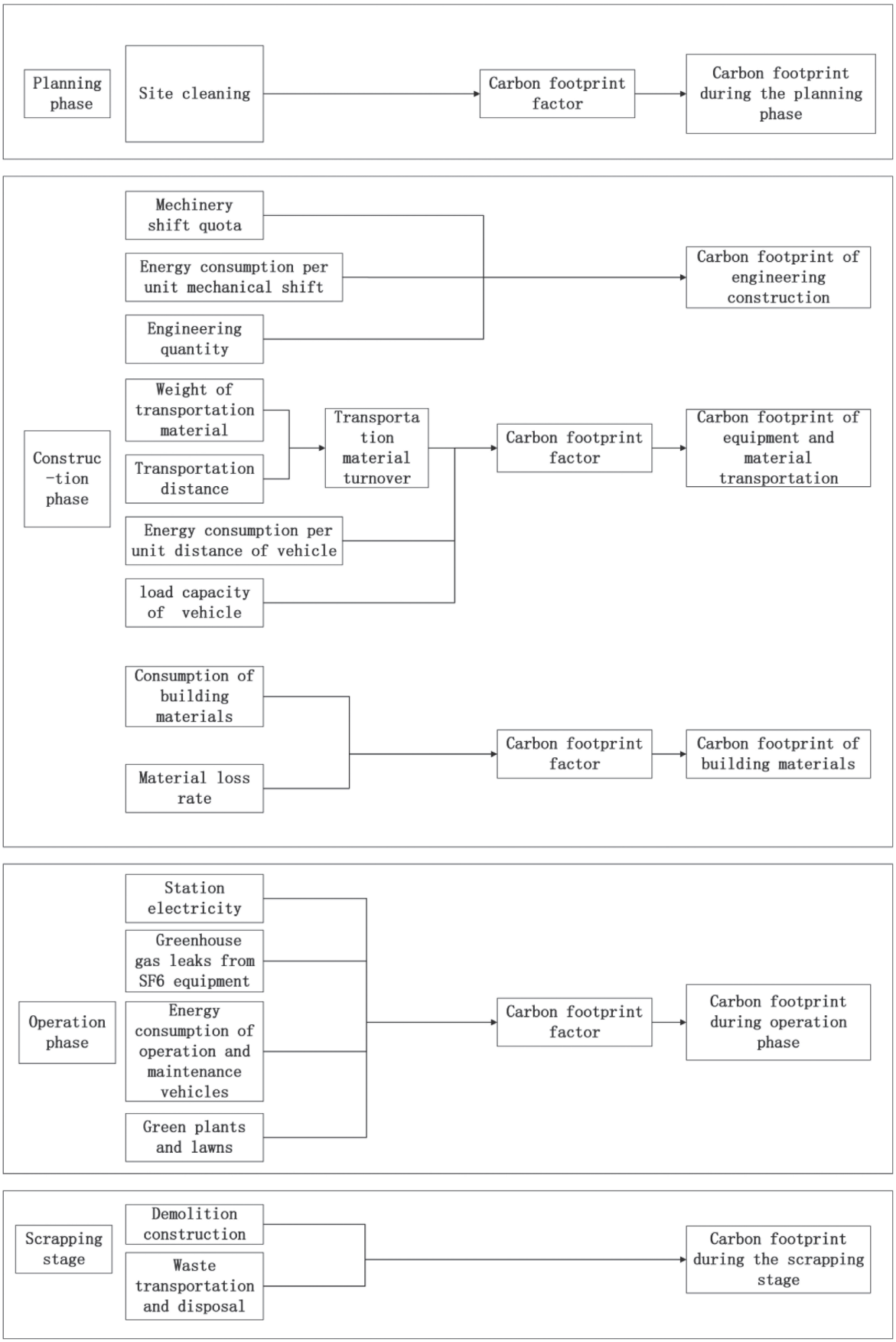

Fig. 1. Carbon footprint composition of prefabricated substation throughout its entire lifecycle.

(4) We have constructed a BA-ELM substation carbon footprint prediction model and trained the model parameters based on sample data, which can effectively improve the accuracy of the BA-ELM model in predicting the carbon footprint of substations.

Materials and Methods

Carbon Footprint Calculation Method for Prefabricated Cabin Substations

The carbon footprint of a prefabricated substation throughout its entire life cycle includes the carbon footprint generated during the planning phase, construction phase, construction phase, operation phase, and scrapping phase:

$$C = C_C + C_J + C_Y + C_F \quad (1)$$

Among them, C_C, C_J, C_Y, and C_F are the carbon footprints generated during the four stages of preparation, construction, operation, and scrapping, respectively.

(1) Carbon footprint during the planning phase

The carbon footprint during the planning phase mainly comes from the energy and materials consumed during site cleaning. Referring to relevant research, it can be calculated at 105 kg CO_2e/m^2.

(2) Carbon footprint during the construction phase

The carbon footprint of a prefabricated substation during the construction phase includes the carbon footprint generated by engineering construction, equipment and material transportation, and building materials:

$$C_J = C_S + C_T + C_M \quad (2)$$

Among them, C_J is the carbon footprint during the construction phase of prefabricated substations, C_S is the carbon footprint of engineering construction, C_T is the carbon footprint of equipment and material transportation, and C_M is the carbon footprint of building materials.

The carbon footprint of engineering construction is mainly generated by the energy consumption of various construction machines during operation. Therefore, the engineering carbon footprint can be calculated through the engineering quantity, machinery shift quota, and energy consumption per unit mechanical shift:

$$C_S = \sum_{i=1}^{n} Q_i \cdot MT_i \cdot ME_i \cdot CF_i \quad (3)$$

Among them, Q_i is the engineering quantity of the i-th process, MT_i is the machinery shift quota, ME_i is the energy consumption per unit mechanical shift, and CF_i is the carbon footprint factor.

The carbon footprint of equipment and material transportation refers to the carbon emissions generated by the energy consumption of vehicles during transportation.

$$C_T = \sum_{i=1}^{n}\sum_{j=1}^{m} W_i \cdot D_i / CAW_j \cdot V_j \cdot CF_j \quad (4)$$

Among them, W_i is the weight of the i-th type of transportation material (or equipment), D_i i is the transportation distance, and CAW_j is the load capacity of the j-th type of vehicle, V_j is the energy consumption per unit distance of the j-th type of vehicle, and CF_j is the carbon footprint factor.

The carbon footprint of building materials mainly comes from the production process of building materials, and the composition of the carbon footprint of building materials is:

$$C_M = \sum_{i=1}^{n} M_i \cdot (1 + l_i) \cdot CF_i \quad (5)$$

Among them, M_i is the consumption of building materials, l_i is the material loss rate, and CF_i is the carbon footprint factor.

(3) Carbon footprints during the operation phase

Carbon footprints during the operation phase mainly include carbon emissions generated by station electricity, greenhouse gas leaks from SF_6 equipment, carbon emissions generated by the energy consumption of operation and maintenance vehicles, and carbon emissions absorbed by green plants and lawns.

The carbon emission factor for station electricity adopts the national average carbon dioxide emission factor for electricity (0.5568 kg CO_2/kWh) as stated in the Announcement on the Release of Carbon Dioxide Emission Factors for Electricity in 2021 by the Ministry of Ecology and Environment and the National Bureau of Statistics.

The SF_6 gas dissipation refers to the typical design scheme of a 110 kV substation. The SF_6 gas content in the GIS equipment is 2.25 t. Calculated based on an annual leakage of 0.5% (0.01125 t/year), the global warming potential (GWP) of SF_6 is 23900 times that of CO_2, and the equivalent carbon emissions are 268.875 t.

Carbon emissions generated by the energy consumption of maintenance vehicles:

$$C_R = \sum_{i=1}^{n} VE_i \cdot CF_i \quad (6)$$

Among them, VE_i is the energy consumption of operation and maintenance vehicles and CF_i is the carbon footprint factor.

The carbon sink of green plants and lawns can refer to -13.425 $kgCO_2e/(m^2 \cdot a)$ and -1.15 $kgCO_2e/(m^2 \cdot a)$.

(4) Carbon footprint during the scrapping stage

The carbon footprint during the scrapping stage refers to existing research results and is simplified by 10% of the carbon footprint during the construction stage.

Gray Relational Analysis

Gray Relational Analysis (GRA) determines the correlation between factors based on their similarity

and dissimilarity, and this degree of correlation is called the Gray Relational degree. According to the gray correlation degree, the correlation of factors can be sorted to screen out factors with higher correlation further. The steps are as follows:

Step 1: Determine the reference sequence and the comparison sequence in the sample data, t = 1, 2, 3, …, m; i = 1, 2, 3, …, n. Take the carbon footprint sequence of prefabricated cabin substations as the reference sequence and the influencing factor sequences (construction energy consumption, transportation energy consumption, station electricity, etc.) as the comparison sequences.

Step 2: Perform dimensionless data processing:

$$x_i'(t) = \frac{x_i(t) \bullet m}{\sum_{t=1}^{m} x_i(t)} \tag{7}$$

Step 3: Calculate the correlation coefficient between the comparison sequence and the reference sequence:

$$\xi_i(t) = \frac{\min\limits_i \min\limits_t |r_0(t) - x_i'(t)| + \rho \max\limits_i \max\limits_t |r_0(t) - x_i'(t)|}{|r_0(t) - x_i'(t)| + \rho \max\limits_i \max\limits_t |r_0(t) - x_i'(t)|} \tag{8}$$

Among them, ρ is the resolution coefficient, which has a value range of (0,1), generally taken as 0.5.

Step 4: Calculate correlation:

$$\gamma_i = \frac{1}{m} \sum_{t=1}^{m} \xi_i(t) \tag{9}$$

Bat Algorithm

As a population-based intelligent optimization algorithm, the bat algorithm optimizes calculations by simulating the foraging behavior of bats. The update process of the bat algorithm for position and velocity is as follows:

$$f_i = f_{min} + (f_{max} - f_{min})\lambda \tag{10}$$

$$v_i^t = v_i^{t-1} + (x_i^{t-1} - x^*) f_i \tag{11}$$

$$x_i^t = x_i^{t-1} + v_i^t \tag{12}$$

Among them, f_i, f_{min}, and f_{max} represent the pulse frequency of the i-th bat, as well as the minimum and maximum values of the pulse frequency, respectively. λ is a random variable between 0 and 1. v_i^t, x_i^t represent the flight speed and position of the i-th bat individual. x^* represents the global optimal value of bat position [29, 30].

To improve local search capability, update the current position when the bat approaches the global optimum:

$$x_i^t = x_{best} + rand(-1,1) A_i^t \tag{13}$$

Among them, x_{best} is the current global optimal solution of the bat population, and A_i^t is the sound wave loudness at time t.

Bats increase the probability of discovering prey by varying the volume and frequency of sound waves while searching for them. At the beginning of the search, bats emit sound waves with high loudness and low frequency, thus conducting a global search over a large area. As the search range decreases and the prey gets closer, bats will increase their frequency and decrease their loudness to search for the location of the target prey more accurately. During the search process, the changes in the loudness and frequency of bat sound waves are as follows [31, 32]:

$$A_i^{t+1} = \alpha A_i^t \tag{14}$$

$$r_i^{t+1} = r_i^0 (1 - e^{-kt}) \tag{15}$$

Among them, α is a random number within the range of (0, 1), r_i^{t+1} is the pulse frequency at time t+1, r_i^0 is the initial pulse frequency of bat i, k is the bat pulse frequency enhancement coefficient, k > 0.

In Table 8, the maximum and minimum pulse frequencies of bats are 6 and 0, respectively. The number of bats is 65, the maximum loudness is 1.5, the initial pulse frequency is 1.2, and the maximum number of iterations is 100. Update the optimal solution of the bat algorithm based on the carbon footprint prediction error value until the prediction accuracy requirement is met.

Using the Mean Absolute Percentage Error (MAPE) as the loss function for model training to evaluate the effectiveness of model learning

$$\text{MAPE} = \frac{1}{n} \sum_{i=1}^{n} \left| \frac{\hat{y}_i - y_i}{y_i} \right| \times 100\%$$

Among them, $\hat{y}_i$ represents the predicted value, y_i represents the actual value, and n represents the number of predicted points.

Extreme Learning Machine

Extreme Learning Machine (ELM) is a type of neural network with a single hidden layer structure. After initialization, the input weights generally do not need to be adjusted again. Compared with traditional neural networks that require a large number of training samples, ELM has higher flexibility and can adapt to complex machine learning needs. It has the advantages of fast convergence and is not easily trapped in local optima.

For the given N samples , the number of input layer nodes is k, and the number of hidden layer nodes is m. The ELM neural network can be represented as:

$$\sum_{i=1}^{m} \beta_i \, g(\langle w_i, x_i \rangle + b_i) = o_j \quad \text{j} = 1, 2, 3, \ldots, \text{N} \tag{16}$$

Among them, g(x) is the Sigmoid activation function, w_i is the weight between the i-th hidden node and the input node, b_i is the bias of the i-th hidden node, β_i is the weight between the i-th hidden node and the output node, and o_j is the output value of ELM.

H represents the output matrix of the ELM hidden layer, β represents the output weight matrix, T represents the expected output matrix, and ELM can be expressed as:

$$H\beta = T \tag{17}$$

By solving Equation 17,

$$\hat{\beta} = H^{+}T \tag{18}$$

Among them, H^{+} is the Moore-Penrose generalized inverse matrix of the hidden layer output matrix H [33–36].

Carbon Footprint Prediction Model for Prefabricated Cabin Substations

Using the carbon footprint data of prefabricated substations as samples, a bat algorithm optimized ELM model (BA-ELM) was constructed. The gray correlation analysis method was used to screen the influencing factors of the substation's carbon footprint, and the BA-ELM prediction model was trained on the carbon footprint sample data. The weights and biases of ELM were iteratively optimized using the bat algorithm to continuously improve the convergence of BA-ELM on the carbon footprint sample data. The trained BA-ELM model was used as an optimization model to predict the carbon footprint data of prefabricated substations.

Empirical Research

Calculation of Carbon Emission Factors

The carbon emission factor cannot be directly obtained and needs to be calculated based on the heating value of unit energy consumption, the carbon content per unit calorific value, and the carbon oxidation rate provided in the "Guidelines for Compilation of Provincial Greenhouse Gas Inventories (2011)". The carbon oxidation rate of liquid fuel is 0.98, the carbon oxidation rate of gas fuel is 0.99, and the carbon oxidation rate of solid fuel varies depending on the type of fuel. The calculation factors for the carbon footprint generated by energy consumption throughout the entire lifecycle of a substation are shown in Table 1.

Carbon Footprint Calculation of Prefabricated Cabin Substation

Select four 110 kV prefabricated cabin substation projects as research objects, with construction capacities of 2×50 MVA, 2×50 MVA, 2×63 MVA, and 2×50 MVA for projects 1, 2, 3, and 4, respectively. According to the energy carbon footprint factor calculated above and the power carbon emission factor released in the Announcement of the Ministry of Ecology and Environment and the National Bureau of Statistics on the Release of Carbon Dioxide Emission Factors for Electricity in 2021, the warming potential value of SF_6 is calculated at 23900. The carbon footprint results of four prefabricated cabin substation projects in the planning, construction, operation, and scrapping stages are shown in Table 2 and Table 3.

Table 1. Calculation Table of Energy Consumption Carbon Footprint Factor.

Classification	Types of fuel	Heating value of unit energy consumption (kJ/kg)	Carbon content per unit calorific value (tC/TJ)	Carbon oxidation rate	Unit calorific value CO_2 emission factor ($kgCO_2/kg$)
solid fuel	standard coal	29307	26.37	0.94	2.664
	anthracite	30564	27.4	0.94	2.886
	bituminous coal	37200	26.1	0.93	3.311
	lignite	27214	28	0.96	2.682
	coke	28435	29.5	0.93	2.860
liquid fuel	crude oil	41816	20.1	0.98	3.020
	fuel oil	41816	21.1	0.98	3.170
	gasoline	43070	18.9	0.98	2.925
	diesel oil	42552	20.2	0.98	3.089
	general kerosene	43070	19.6	0.98	3.033
	LPG liquefied petroleum gas	50179	17.2	0.98	3.101
	Refinery Gas	45998	18.2	0.98	3.008
gas fuel	natural gas	38931	15.3	0.99	2.162

Table 2. Carbon footprint analysis table for each stage of the substation (unit: tCO_2e).

Stage	Name	Project 1	Project 2	Project 3	Project 4
planning stage	planning stage carbon footprint	0.00	0.00	0.00	0.00
construction stage	construction carbon footprint	64.09	67.67	68.00	63.35
	transportation carbon footprint	505.11	454.60	518.95	491.27
	material carbon footprint	42507.55	43012.14	42179.93	42267.25
operation stage	station electricity carbon footprint	2438.78	3048.48	3170.42	2682.66
	SF_6 dissipation carbon footprint	13443.75	13443.75	13443.75	13443.75
	operation and maintenance vehicles carbon footprint	2242.01	2309.27	2398.95	2286.85
	green plants and lawns carbon footprint	-69.96	-42.62	-48.77	-59.83
scrapping stage	scrapping carbon footprint	4307.68	4353.44	4276.69	4282.19
total		65439.02	66646.73	66007.93	65457.49

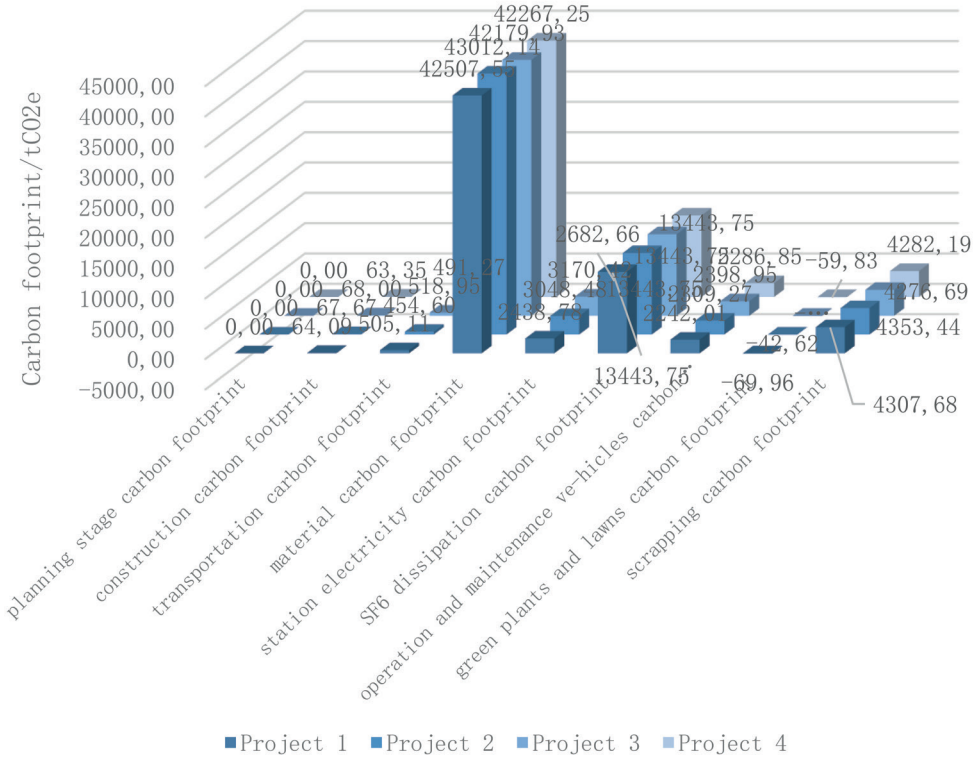

Fig. 2. Carbon footprint of each stage of the substation.

The carbon footprint during the planning stage is mainly due to site clearance. The project is located in the urban area, and there are no structures or obstacles that need to be removed from the construction site. Therefore, the carbon footprint during the planning phase is not included.

The carbon footprint during the construction stage mainly includes the carbon footprint generated during the production process of materials such as concrete and steel bars, the carbon footprint during the production and installation of transformers and GIS equipment, and the carbon footprint during the use of construction machinery and transportation of materials and equipment.

The carbon footprint of station electricity in the operation stage is calculated based on the electricity carbon footprint factor, the SF_6 dissipation carbon footprint is calculated based on the SF_6 global warming potential (GWP), the carbon footprint of operation and maintenance vehicles is calculated based on the energy carbon footprint factor, and the carbon

Table 3. Main carbon footprint of the substation (unit: tCO_2e).

Project	Name	Activity level	Unit	Carbon footprint factor	Factor unit	Carbon footprint	Carbon footprint unit
Project 1	Construction energy consumption	207480	kg	3.089	$kgCO_2/kg$	64.09057	tCO_2e
	Transportation energy consumption	1635200	kg	3.089	$kgCO_2/kg$	505.1133	tCO_2e
	Station electricity	8.76	10000 kWh/year	0.5568	$kgCO_2/kWh$	2438.784	tCO_2e
	Operation and maintenance vehicles	153300	kg	2.925	$kgCO_2/kg$	2242.013	tCO_2e
	Green plants	76.25	m^2	-13.425	$kgCO_2e/(m^2•a)$	-51.1828	tCO_2e
	lawn	326.5	m^2	-1.15	$kgCO_2e/(m^2•a)$	-18.7738	tCO_2e
	concrete	4503.71	m^3	295	$kg\ CO_2e/m^3$	1328.594	tCO_2e
	steel bars	339.14	t	2340	$kg\ CO_2e/t$	793.5876	tCO_2e
	transformers	2	one	27.06	tCO_2e	54.12	tCO2e
	GIS composite appliances	1	set	40331.25	tCO2e	40331.25	tCO_2e
Project 2	Construction energy consumption	219055.2	kg	3.089	$kgCO_2/kg$	67.66615	tCO_2e
	Transportation energy consumption	1471680	kg	3.089	$kgCO_2/kg$	454.602	tCO_2e
	Station electricity	10.95	10000 kWh/year	0.5568	$kgCO_2/kWh$	3048.48	tCO_2e
	Operation and maintenance vehicles	157899	kg	2.925	$kgCO_2/kg$	2309.273	tCO_2e
	Green plants	46.25	m^2	-13.425	$kgCO_2e/(m^2•a)$	-31.0453	tCO_2e
	lawn	201.36	m^2	-1.15	$kgCO_2e/(m_2•a)$	-11.5782	tCO_2e
	concrete	4912.36	m^3	295	$kg\ CO_2e/m^3$	1449.146	tCO_2e
	steel bars	503.26	t	2340	$kg\ CO_2e/t$	1177.628	tCO_2e
	transformers	2	one	27.06	tCO_2e	54.12	tCO_2e
	GIS composite appliances	1	set	40331.25	tCO_2e	40331.25	tCO_2e
Project 3	Construction energy consumption	220147.2	kg	3.089	$kgCO_2/kg$	68.00347	tCO_2e
	Transportation energy consumption	1680000	kg	3.089	$kgCO_2/kg$	518.952	tCO_2e
	Station electricity	11.388	10000 kWh/year	0.5568	$kgCO_2/kWh$	3170.419	tCO_2e
	Operation and maintenance vehicles	164031	kg	2.925	$kgCO_2/kg$	2398.953	tCO_2e
	Green plants	53.26	m^2	-13.425	$kgCO_2e/(m^2•a)$	-35.7508	tCO_2e
	lawn	226.35	m^2	-1.15	$kgCO_2e/(m^2•a)$	-13.0151	tCO_2e
	concrete	3759.26	m^3	295	$kg\ CO_2e/m^3$	1108.982	tCO_2e
	steel bars	286.97	t	2340	$kg\ CO_2e/t$	671.5098	tCO_2e

→

Project	Name	Activity level	Unit	Carbon footprint factor	Factor unit	Carbon footprint	Carbon footprint unit
	transformers	2	one	34.0956	tCO_2e	68.1912	tCO_2e
	GIS composite appliances	1	set	40331.25	tCO_2e	40331.25	tCO_2e
Project 4	Construction energy consumption	205077.6	kg	3.089	$kgCO_2/kg$	63.34847	tCO_2e
	Transportation energy consumption	1590400	kg	3.089	$kgCO_2/kg$	491.2746	tCO_2e
	Station electricity	9.636	10000 kWh/year	0.5568	$kgCO_2/kWh$	2682.662	tCO_2e
	Operation and maintenance vehicles	156366	kg	2.925	$kgCO_2/kg$	2286.853	tCO_2e
	Green plants	64.85	m^2	-13.425	$kgCO_2e/(m^2•a)$	-43.5306	tCO_2e
	lawn	283.54	m^2	-1.15	$kgCO_2e/(m^2•a)$	-16.3036	tCO_2e
	concrete	3956.28	m^3	295	$kg\ CO_2e/m^3$	1167.103	tCO_2e
	steel bars	305.46	t	2340	$kgCO_2e/t$	714.7764	tCO_2e
	transformers	2	one	27.06	tCO_2e	54.12	tCO_2e
	GIS composite appliances	1	set	40331.25	tCO_2e	40331.25	tCO_2e

footprint of green plants and lawns is calculated based on the corresponding negative emission factor.

The carbon footprint during the scrapping stage is simplified to 10% of the carbon footprint during the construction phase.

According to the definition of carbon footprint, it is the sum of greenhouse gas emissions and greenhouse gas removals. According to Table 2 and Fig. 2, it can be seen that only the carbon footprint of green plants and lawns is negative, which is the amount of greenhouse gas removal; all other carbon footprints are greenhouse gas emissions. The material carbon footprint and SF_6 dissipation carbon footprint are the carbon footprints with the highest proportions. Therefore, by optimizing the engineering quantity, improving the production technology level of building materials, and replacing existing GIS equipment with SF_6 free equipment, the carbon footprint of prefabricated cabin substations can be effectively reduced. In addition, by increasing the area of green plants and lawns, the removal of greenhouse gases can also be increased, which can reduce the carbon footprint of prefabricated substations.

Sensitivity Analysis

In order to analyze the impact of changes in indicators of different activity levels on the total carbon footprint of substations, the focus was on analyzing the changes in carbon footprint caused by changes in indicators such as construction energy consumption, transportation energy consumption, station electricity consumption, operation and maintenance vehicles, green plants, lawns, concrete, steel bars, transformers, GIS composite appliances, etc. The results are shown in Table 4. The change in the activity level of GIS composite appliances has the greatest impact on the total carbon footprint. When the activity level of GIS composite appliances increases by 10%, the carbon footprint of substations increases by more than 6%. Project 1 has the highest carbon footprint change rate, which is 6.1632%. For every 10 percentage points increase in station electricity activity level, the total carbon footprint of projects 1, 2, 3, and 4 increases by 0.3727%, 0.4574%, 0.4803%, and 0.4098%, respectively. For every 10 percentage points increase in the activity level of operation and maintenance vehicles, the total carbon footprint of projects 1, 2, 3, and 4 increases by 0.3426%, 0.3465%, 0.3634%, and 0.3494%, respectively. The changes in the usage of materials such as concrete and steel bars have a significant impact on carbon footprint. For every 10 percentage points increase in concrete usage, the total carbon footprint of projects 1, 2, 3, and 4 increases by 0.2030%, 0.2174%, 0.1680%, and 0.1783%, respectively. For every 10 percentage points increase in steel bar usage, the total carbon footprint of projects 1, 2, 3, and 4 increases by 0.1213%, 0.1767%, 0.1017%, and 0.1092%, respectively.

Results and Discussion

Selection of Factors Influencing the Carbon Footprint of Substations Based on Gray Relational Analysis

In order to analyze the main factors affecting the carbon footprint of the prefabricated substation, gray correlation

Table 4. Sensitivity analysis table.

Activity level	Activity level change rate (%)	Total carbon footprint change rate (%)			
		Project 1	Project 2	Project 3	Project 4
Construction energy consumption	-10	-0.0098%	-0.0102%	-0.0103%	-0.0097%
	-5	-0.0049%	-0.0051%	-0.0052%	-0.0048%
	5	0.0049%	0.0051%	0.0052%	0.0048%
	10	0.0098%	0.0102%	0.0103%	0.0097%
Transportation energy consumption	-10	-0.0772%	-0.0682%	-0.0786%	-0.0751%
	-5	-0.0386%	-0.0341%	-0.0393%	-0.0375%
	5	0.0386%	0.0341%	0.0393%	0.0375%
	10	0.0772%	0.0682%	0.0786%	0.0751%
Station electricity	-10	-0.3727%	-0.4574%	-0.4803%	-0.4098%
	-5	-0.1863%	-0.2287%	-0.2402%	-0.2049%
	5	0.1863%	0.2287%	0.2402%	0.2049%
	10	0.3727%	0.4574%	0.4803%	0.4098%
Operation and maintenance vehicles	-10	-0.3426%	-0.3465%	-0.3634%	-0.3494%
	-5	-0.1713%	-0.1732%	-0.1817%	-0.1747%
	5	0.1713%	0.1732%	0.1817%	0.1747%
	10	0.3426%	0.3465%	0.3634%	0.3494%
Green plants	-10	0.0078%	0.0047%	0.0054%	0.0067%
	-5	0.0039%	0.0023%	0.0027%	0.0033%
	5	-0.0039%	-0.0023%	-0.0027%	-0.0033%
	10	-0.0078%	-0.0047%	-0.0054%	-0.0067%
lawn	-10	0.0029%	0.0017%	0.0020%	0.0025%
	-5	0.0014%	0.0009%	0.0010%	0.0012%
	5	-0.0014%	-0.0009%	-0.0010%	-0.0012%
	10	-0.0029%	-0.0017%	-0.0020%	-0.0025%
concrete	-10	-0.2030%	-0.2174%	-0.1680%	-0.1783%
	-5	-0.1015%	-0.1087%	-0.0840%	-0.0891%
	5	0.1015%	0.1087%	0.0840%	0.0891%
	10	0.2030%	0.2174%	0.1680%	0.1783%
steel bars	-10	-0.1213%	-0.1767%	-0.1017%	-0.1092%
	-5	-0.0606%	-0.0883%	-0.0509%	-0.0546%
	5	0.0606%	0.0883%	0.0509%	0.0546%
	10	0.1213%	0.1767%	0.1017%	0.1092%
transformers	-10	-0.0083%	-0.0081%	-0.0103%	-0.0083%
	-5	-0.0041%	-0.0041%	-0.0052%	-0.0041%
	5	0.0041%	0.0041%	0.0052%	0.0041%
	10	0.0083%	0.0081%	0.0103%	0.0083%

→

Activity level	Activity level change rate (%)	Total carbon footprint change rate (%)			
		Project 1	Project 2	Project 3	Project 4
GIS composite appliances	-10	-6.1632%	-6.0515%	-6.1101%	-6.1614%
	-5	-3.0816%	-3.0257%	-3.0550%	-3.0807%
	5	3.0816%	3.0257%	3.0550%	3.0807%
	10	6.1632%	6.0515%	6.1101%	6.1614%

analysis was conducted on multiple indicators such as construction energy consumption, transportation energy consumption, station electricity consumption, operation and maintenance vehicles, green plants, lawns, concrete, steel bars, transformers, GIS composite appliances, etc., to calculate the correlation between the indicators and the carbon footprint of the prefabricated substation. Sort the influencing factors based on the correlation index and select the main influencing factors of the carbon footprint of prefabricated cabin substations as input variables for the carbon footprint prediction model.

The data obtained by dimensionless processing of the influencing factor indicators are shown in Table 5. The difference sequence between the comparison sequence (influencing factors) and the reference sequence (carbon footprint) was further calculated, and the results are shown in Table 6. The correlation coefficient and correlation degree of the influencing factors were calculated based on the difference sequence, and the results are shown in Table 7 and Fig. 3.

In Fig. 3, the correlation between transformers, GIS composite appliances, and carbon footprint is the highest at 0.976. The factors that have a significant impact on carbon footprint include operation and maintenance vehicles (0.925), construction energy consumption (0.897), transportation energy consumption (0.837), station electricity consumption (0.702), and concrete (0.684). Green plants and lawns can effectively eliminate carbon emissions and have a negative impact on carbon footprint. However, due to their small area and low carbon footprint factor, their impact on carbon footprint is limited. By further expanding the area of green plants and lawns in the station area and planting plant species with higher carbon footprint factors, the absorption of carbon emissions can be improved.

Based on the analysis of the factors affecting the carbon footprint of prefabricated cabin substations, seven variables, including transformers, GIS composite electrical appliances, operation and maintenance vehicles, construction energy consumption, transportation energy consumption, station electricity consumption, and concrete, were selected as

Table 5. Dimensionalization calculation results of influencing factors.

Influence factor	Construc-tion energy consump-tion	Transpor-tati-on energy con-sumption	Stati-on elect-ricity	Operati-on and maint-en-ance vehicles	Green plants	lawn	Conc-rete	steel bars	Transfo-rmers	GIS compos-ite appli-ances
Project 1	0.974	1.026	0.860	0.971	1.268	1.258	1.052	0.945	1.000	1.000
Project 2	1.029	0.923	1.075	1.000	0.769	0.776	1.147	1.403	1.000	1.000
Project 3	1.034	1.054	1.118	1.039	0.885	0.872	0.878	0.800	1.000	1.000
Project 4	0.963	0.998	0.946	0.990	1.078	1.093	0.924	0.852	1.000	1.000

Table 6. The difference sequence between the compared sequence and the reference sequence.

Difference sequence	Construction energy con-sumption	Transportati-on energy consumption	Station electri-city	Operation and mainten-ance vehicles	Green plants	lawn	Concrete	steel bars	Trans-formers	GIS com-posite ap-pliances
Project 1	0.019	0.032	0.133	0.022	0.274	0.265	0.058	0.048	0.007	0.007
Project 2	0.017	0.088	0.064	0.012	0.243	0.235	0.135	0.391	0.012	0.012
Project 3	0.032	0.052	0.116	0.037	0.116	0.129	0.124	0.202	0.002	0.002
Project 4	0.030	0.004	0.047	0.003	0.085	0.099	0.070	0.142	0.007	0.007

Table 7. Correlation coefficient of carbon footprint influencing factors.

Correlation coefficient	Construction energy consumption	Transportation energy consumption	Station electricity	Operation and maintenance vehicles	Green plants	lawn	Concrete	steel bars	Transformers	GIS composite appliances
Project 1	0.921	0.866	0.601	0.906	0.420	0.429	0.777	0.811	0.975	0.975
Project 2	0.928	0.695	0.761	0.953	0.451	0.458	0.597	0.336	0.953	0.953
Project 3	0.867	0.798	0.633	0.849	0.633	0.608	0.618	0.497	1.000	1.000
Project 4	0.874	0.989	0.813	0.993	0.705	0.669	0.744	0.585	0.977	0.977

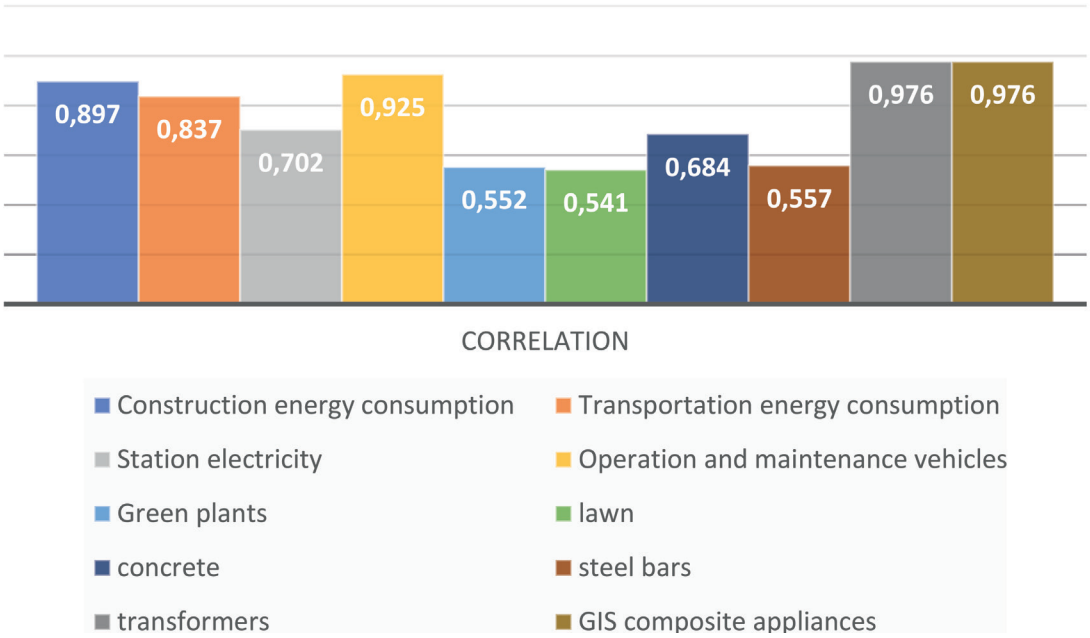

Fig. 3. The correlation between carbon footprint and influencing factors of prefabricated cabin substations.

the main influencing factors of carbon footprint and used as input variables for the BA-ELM prediction model.

Parameter Setting and Model Construction

In order to verify the accuracy of the BA-ELM model in predicting the carbon footprint of prefabricated substations, sample data was used to train the BA-ELM model, and the four items in this paper were used as the test set for prediction validation. The main parameter settings of the model are shown in Table 8. The number of bats is set to 65 to improve the efficiency and convergence speed of the algorithm. The maximum number of iterations is set to 100 to avoid overfitting the algorithm and enhance the model's generalization ability. The hidden layer node is set to 12 in order to obtain effective information on influencing factors to the maximum extent possible while avoiding excessive model complexity and improving the accuracy of carbon footprint prediction [25].

In Fig. 4, as the model training process progresses, the loudness of the bat in the BA algorithm continuously decreases [26], the pulse frequency continuously increases, and the accuracy of the search algorithm continues to improve. Therefore, the fitting accuracy of the BA-ELM prediction model on carbon footprint sample data continues to improve. At the 57th iteration, the prediction error of the model decreased to 1.31%, and thereafter, with the increase of iterations, the error rate did not show a significant decrease. This indicates that the model parameters in the 57th iteration are the current global optimal solution of BA-ELM.

Research on Substation Carbon Footprint Prediction Based on BA-ELM Model

Empirical prediction studies were conducted on the carbon footprint of the four prefabricated cabin substations mentioned above. The prediction results are shown in Table 9 and Fig. 5, and the prediction errors are

Table 8. BA-ELM model parameter setting.

Model	Parameter	Value
BA	Maximum pulse frequency	6
	Minimum pulse frequency	0
	Number of bats	65
	Maximum loudness	1.5
	Initial pulse frequency	1.2
	Maximum number of iterations	100
ELM	Number of hidden layer nodes	12
	kernel function	sig

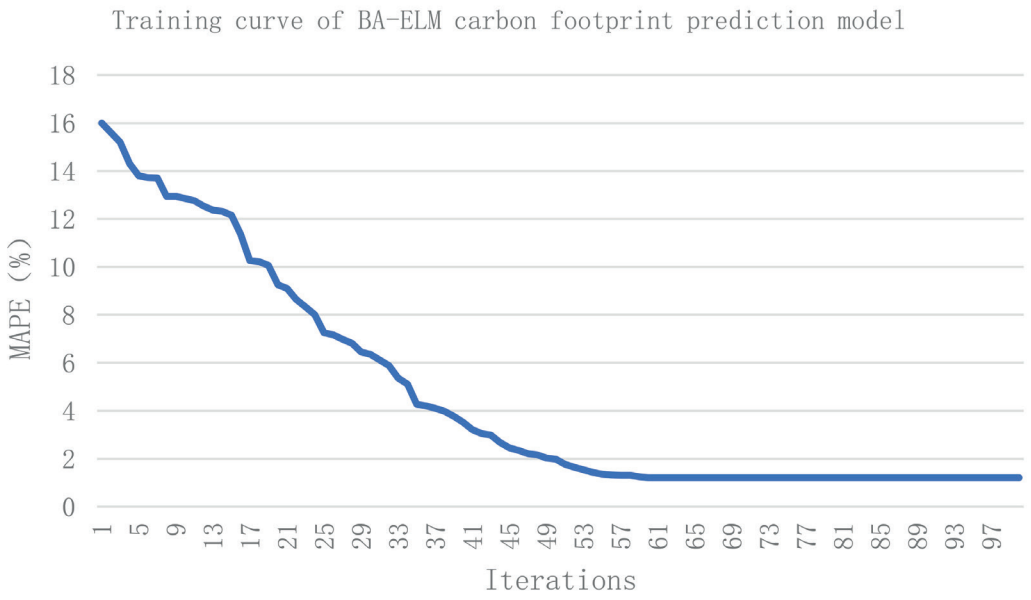

Fig. 4. Training curve of BA-ELM carbon footprint prediction model.

Table 9. Prediction results of BA-ELM prediction model for carbon footprint of substations.

Stage	Name	Project 1		Project 2		Project 3		Project 4	
		Actual	Predict	Actual	Predict	Actual	Predict	Actual	Predict
planning stage	planning stage carbon footprint	0	0	0	0	0	0	0	0
construction stage	construction carbon footprint	64.09	65.26	67.67	66.25	68	67.68	63.35	64.28
	transportation carbon footprint	505.11	501.23	454.6	449.36	518.95	526.36	491.27	503.16
	material carbon footprint	42507.55	42019.32	43012.14	42895.32	42179.93	41846.35	42267.25	42031.26
operation stage	station electricity carbon footprint	2438.78	2553.21	3048.48	3125.89	3170.42	3216.25	2682.66	2746.85
	SF6 dissipation carbon footprint	13443.75	13021.87	13443.75	12945.26	13443.75	12983.48	13443.75	13217.78

Stage	Name	Project 1		Project 2		Project 3		Project 4	
		Actual	Predict	Actual	Predict	Actual	Predict	Actual	Predict
	operation and maintenance vehicles carbon footprint	2242.01	2412.35	2309.27	2215.68	2398.95	2315.26	2286.85	2325.48
	green plants and lawns carbon footprint	-69.96	-67.23	-42.62	-41.06	-48.77	-49.26	-59.83	-60.15
scrapping stage	scrapping carbon footprint	4307.68	4336.25	4353.44	4312.71	4276.69	4198.46	4282.19	4267.38
total		65439.02	64842.26	66646.73	65969.41	66007.93	65104.58	65457.49	65096.04

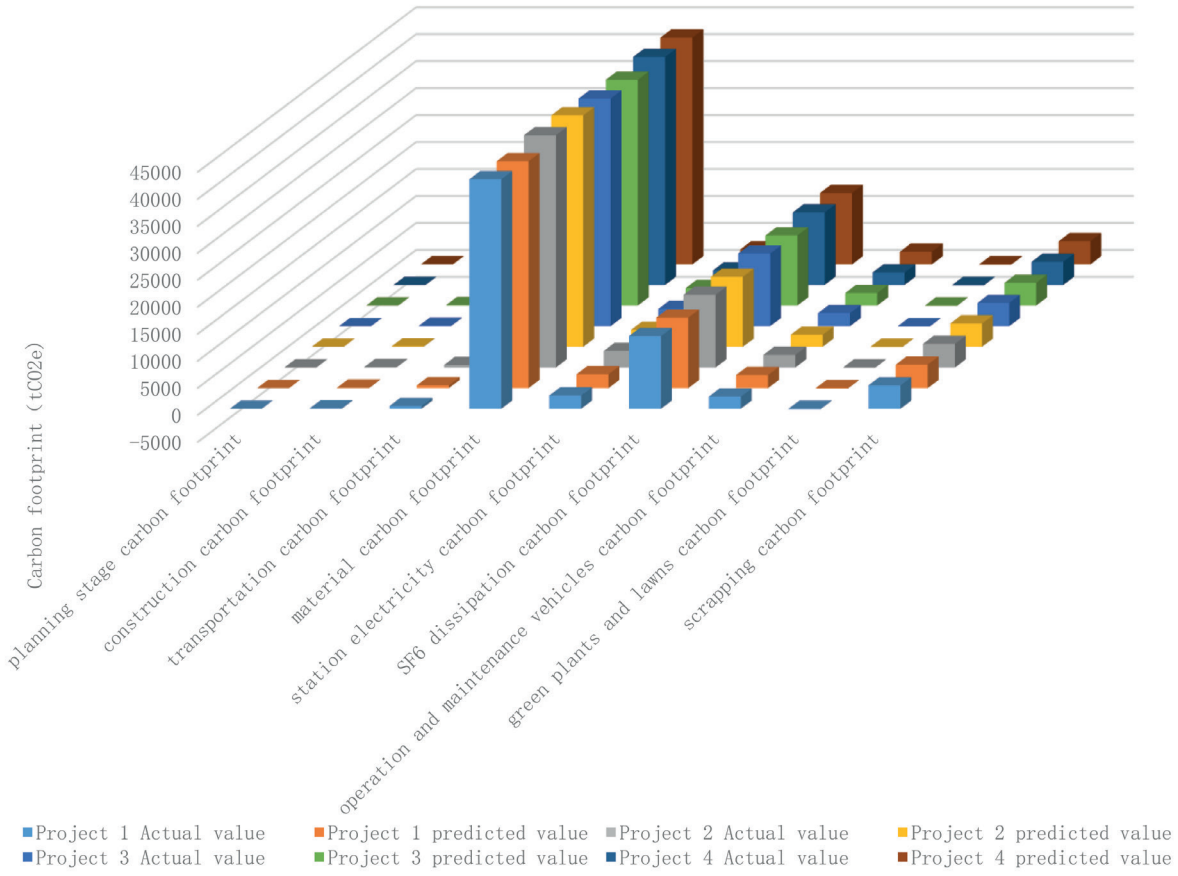

Fig. 5. Prediction results of BA-ELM prediction model for carbon footprint of substations.

shown in Table 10 and Fig. 6. It can be seen that the total carbon footprint prediction errors of the four projects are all below 1.50%, achieving high prediction accuracy. The total carbon footprint prediction error of Project 3 is the largest, at -1.37%, while the total carbon footprint prediction error of Project 4 is the smallest, at -0.55% [13].

Among them, the prediction error of the carbon footprint of transportation vehicles is relatively large, with errors of 7.60%, -4.05%, -3.49%, and 1.69% for the four projects, respectively. The material carbon footprint accounts for the highest proportion of the total carbon footprint, and the prediction accuracy of the material carbon footprint for the four projects is relatively high, with prediction errors of -1.15%, -0.27%, -0.79%, and -0.56%, respectively [29]. The SF_6 carbon footprint is relatively large, with each project exceeding 10,000 tCO_2e. The prediction errors of SF_6 carbon footprint are controlled within a reasonable range, with prediction errors of -3.14%, -3.71%, -3.42%,

Table 10. Prediction error of BA-ELM model.

Deviation	Project 1	Project 2	Project 3	Project 4
planning stage carbon footprint	0	0	0	0
construction carbon footprint	1.83%	-2.10%	-0.47%	1.47%
transportation carbon footprint	-0.77%	-1.15%	1.43%	2.42%
material carbon footprint	-1.15%	-0.27%	-0.79%	-0.56%
station electricity carbon footprint	4.69%	2.54%	1.45%	2.39%
SF6 dissipation carbon footprint	-3.14%	-3.71%	-3.42%	-1.68%
operation and maintenance vehicles carbon footprint	7.60%	-4.05%	-3.49%	1.69%
green plants and lawns carbon footprint	-3.90%	-3.66%	1.00%	0.53%
scrapping carbon footprint	0.66%	-0.94%	-1.83%	-0.35%
total	-0.91%	-1.02%	-1.37%	-0.55%

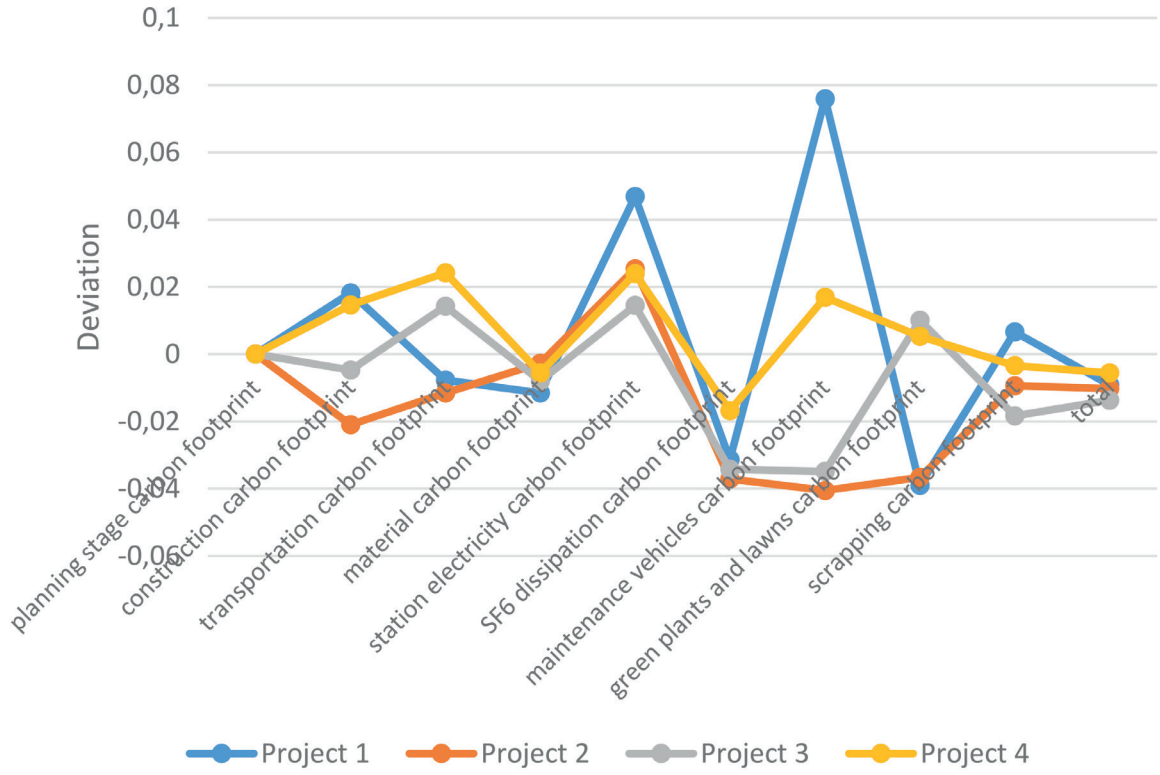

Fig. 6. Prediction error of BA-ELM model.

and -1.68% for the four projects, respectively. For the carbon footprint of green plants and lawns, the prediction errors of the four projects are -3.90%, -3.66%, 1.00%, and 0.53%, respectively, indicating that the BA-ELM model can accurately predict negative carbon emissions (carbon removal) and plays an important role in predicting the carbon footprint of prefabricated substations [30].

Comparison of Model Effects

Compared with the prediction performance of BP neural network (BPNN) and extreme learning machine (ELM), the results are shown in Table 11. The carbon footprint prediction stability of the ELM model is poor, and the prediction error of ELM on project 3 is the largest

Table 11. Comparison of Model Effects.

Prediction model	Project 1	Project 2	Project 3	Project 4
BPNN	3.25%	-2.18%	3.19%	-1.98%
ELM	-2.69%	-3.98%	4.59%	0.87%
BA-ELM	-0.91%	-1.02%	-1.37%	-0.55%

(4.59%). The stability of the BPNN model is better than ELM, but the prediction error is still relatively large. BA-ELM has high stability and prediction accuracy, and its prediction performance is significantly better than BPNN and ELM.

Conclusions

In order to track and evaluate the carbon footprint of a prefabricated substation throughout its entire life cycle, it is divided into four stages: the planning stage, the construction stage, the operation stage, and the scrapping stage. Different types of carbon emissions are calculated, including direct carbon emissions, carbon emissions generated by energy consumption, and carbon emissions generated by material production. The carbon removal amount of green plants, lawns, etc. is considered. A method for calculating the carbon footprint of a prefabricated substation throughout its entire life cycle is proposed, and a BA-ELM carbon footprint prediction model is constructed to predict the carbon footprint of the prefabricated substation. The conclusions drawn are as follows:

(1) The carbon footprint during the construction and operation phases accounts for over 90% of the total lifecycle carbon footprint of prefabricated substations. To control and reduce the carbon footprint of prefabricated substations, it is necessary to reduce energy consumption, use low-carbon and environmentally friendly materials, and adopt advanced production processes. On the other hand, by expanding the planting area of green plants and lawns, carbon removal can be increased, thereby effectively reducing the carbon footprint of substations;

(2) The global warming potential (GWP) of SF_6 is 23900, and its greenhouse effect is much greater than that of CO_2 of the same mass. SF_6 is also a commonly used medium in substation equipment. By using fluorine-free new circuit breakers instead of traditional ones, the carbon emissions of prefabricated substations can be effectively controlled while improving the safety and stability of the system, making it easier to operate and maintain the substations;

(3) The carbon footprint of station electricity is an important component of the carbon footprint of prefabricated cabin substations. It can be effectively reduced by adopting energy-saving equipment, optimizing the layout of electrical equipment in the station, strengthening insulation functions, and using clean energy such as rooftop photovoltaics to meet the demand for station electricity;

(4) Strengthen the monitoring of carbon emissions in prefabricated substations, especially for greenhouse gases with high GWP, such as SF_6, whose greenhouse effect is significant. SF_6 gas in GIS and other equipment should be monitored, the leakage of SF_6 gas should be recorded, and timely measures should be taken to reduce carbon emissions in prefabricated substations;

(5) The constructed BA-ELM substation carbon footprint prediction model, based on sample data to train the model parameters, can effectively improve the accuracy of the BA-ELM model in predicting the carbon footprint of substations, providing a reference for carbon footprint prediction and control of prefabricated cabin substations.

Specifically for the management of prefabricated substations, the main recommendations include: optimizing the substation building scheme in terms of architectural design, reducing the building area, applying photovoltaic building integration technology, and achieving permanent CO_2 storage. In terms of equipment selection, choose more environmentally friendly equipment. Using natural ester-insulated oil transformers and environmentally friendly gas GIS equipment, the carbon emissions of the equipment are significantly reduced by avoiding or reducing the use of SF_6 gas. In terms of daily operation, improve the energy utilization efficiency within the station, promote the application of high-efficiency transformers and capacitors, and reduce equipment operating losses; configure a substation carbon emission monitoring system to monitor and manage energy consumption in real-time, conduct substation carbon footprint prediction; and reduce substation carbon emissions.

This article establishes a method for calculating, predicting, and evaluating the carbon footprint of prefabricated substations and conducts empirical research on the carbon footprint of prefabricated substations, proposing suggestions for energy conservation and carbon reduction in prefabricated substations. Under the dual carbon background, the research results have a positive role and practical significance in establishing low-carbon intelligent substations and accelerating the construction of new power systems.

Acknowledgments

This work was supported by China Southern Power Grid Company Limited Technology projects: Research on the Economic Mechanism of Prefabricated Warehouse Substations under the Dual Carbon Background.

Conflict of Interest

The authors declare no conflict of interest.

References

1. ZHAO X.B., DU D. Forecasting carbon dioxide emissions. Journal of Environmental Management. **160**, 39, **2015**.
2. JIN Y.K., SHARIFI A., LI Z.S., CHEN S.R., ZENG S.Z., ZHAO S.L. Carbon emission prediction models: A review. Science of the Total Environment. **927**, 172319, **2024**.
3. ZHANG Y.J., LAN M.H., ZHAO Y.P., SU Z., HAO Y., DU H. Regional carbon emission pressure and corporate green innovation. Applied Energy. **360**, 122625, **2024**.
4. ZHANG C., ZHANG M.M. Wavelet-based neural network with genetic algorithm optimization for generation prediction of PV plants. Energy Reports. **8**, 10976, **2022**.
5. ZHANG M.M., ABDULLA-AL KAFY., XIAO P.N., HAN S.Y., ZOU S.J., SAHA M., ZHANG C., TAN S.K. Impact of urban expansion on land surface temperature and carbon emissions using machine learning algorithms in Wuhan, China. Urban Climate. **47**, 101347, **2022**.
6. WANG A., ZHANG M.M., CHEN E.Q., ZHANG C., HAN Y.J. Impact of seasonal global land surface temperature (LST) change on gross primary production (GPP) in the early 21st century. Sustainable Cities and Society. **110**, 105572, **2024**.
7. XU C., HUANG G.L., ZHANG M.M. Comparative Analysis of the Seasonal Driving Factors of the Urban Heat Environment Using Machine Learning: Evidence from the Wuhan Urban Agglomeration, China, 2020. Atmosphere. **15** (6), 671, **2024**.
8. LIANG J.S., ZHANG M.M., YIN Z.Q., NIU K.R., LI Y., ZHI K.T., HUANG S.N., YANG J., XU M. Tripartite evolutionary game analysis and simulation research on zero-carbon production supervision of marine ranching against a carbon-neutral background. Frontiers in Ecology and Evolution. **11**, 1119048, **2023**.
9. TAN S.K., ZHANG M.M., WANG A.O., ZHANG X.S., CHEN T.C. How do varying socio-economic driving forces affect China's carbon emissions? New evidence from a multiscale geographically weighted regression model. Environmental Science and Pollution Research. **28**, 41242, **2021**.
10. LIU T., WU Z., CHEN C., CHEN H., ZHOU H.Y. Carbon Emission Accounting during the Construction of Typical 500 kV Power Transmissions and Substations Using the Carbon Emission Factor Approach. Buildings. **14** (1), 145, **2024**.
11. ZHAO S.Z., ZHU Y.X., LOU P., HU Y.Y., XU C.G., CHEN Y.H. Optimization Model of Substation Building Envelope-Renewable Energy Utilization Based on Life-Cycle Minimum Carbon Emissions. Buildings. **13** (7), 1602, **2023**.
12. LIU X.G., ZHANG J., HU Y.Q., LIU J., DING S.J., ZHAO G.W., ZHANG Y., LI J.W., NIE Z.B. Carbon Emission Evaluation Method and Comparison Study of Transformer Substations Using Different Data Sources. Buildings. **13** (4), 1106, **2023**.
13. ARYAI V., GOLDSWORTHY M. Real-time high-resolution modelling of grid carbon emissions intensity. Sustainable Cities and Society. **104**, 105316, **2024**.
14. CHEN X.M., OU Y.T. Carbon emission accounting for power transmission and transformation equipment: An extended life cycle approach. Energy Reports. **10**, 1369, **2023**.
15. LIAN W.W., SUN X.Y., WANG Y.X., DUAN H.M., GAO T.M., YAN Q. The mechanism of China's renewable energy utilization impact on carbon emission intensity: Evidence from the perspective of intermediary transmission. Journal of Environmental Management. **350**, 119652, **2024**.
16. WEI W., WU X., LI J., JIANG X.Y., ZHANG P., ZHOU S.L., ZHU H., LIU H.Z., CHEN H.P., GUO J.L., CHEN G.Q. Ultra-high voltage network induced energy cost and carbon emissions. Journal of Cleaner Production. **178**, 276, **2018**.
17. DANESHZAND F., COKER P.J., POTTER B., SMITH S. EV smart charging how tariff selection influences grid stress and carbon reduction. Applied Energy. **348**, 121482, **2023**.
18. WANG Y., YAN Q., LUO Y.F., ZHANG Q. Carbon abatement of electricity sector with renewable energy deployment: Evidence from China. Renewable Energy. **210**, 1, **2023**.
19. DESIDERI U., PROIETTI S., ZEPPARELLI F., SDRINGOLA P., BINI S. Life Cycle Assessment of a ground-mounted 1778 kWp photovoltaic plant and comparison with traditional energy production systems. Applied Energy. **97** (SI), 930, **2012**.
20. SINGH B., MUKHERJEE V., TIWARI P. Genetic algorithm for impact assessment of optimally placed distributed generations with different load models from minimum total MVA intake viewpoint of main substation. Renewable & Sustainable Energy Reviews. **57**, 1611, **2016**.
21. RUIZ-MENDOZA B.J., SHEINBAUM-PARDO C. Electricity sector reforms in four Latin-American countries and their impact on carbon dioxide emissions and renewable energy. Energy Policy. **38** (11), 6755, **2010**.
22. SHAFFER B., TARROJA B., SAMUELSEN S. Dispatch of fuel cells as Transmission Integrated Grid Energy Resources to support renewables and reduce emissions. Applied Energy. **148**, 178, **2015**.
23. LI Y.W., YANG X.X., DU E.S., LIU Y.L., ZHANG S.X., YANG C., ZHANG N., LIU C. A review on carbon emission accounting approaches for the electricity power industry. Applied Energy. **359**, 122681, **2024**.
24. MILLER G.J., NOVAN K., JENN A. Hourly accounting of carbon emissions from electricity consumption. Environmental Research Letters. **17** (4), 044073, **2022**.
25. WEI W.D., ZHANG P.F., YAO M.T., XUE M., MIAO J.W., LIU B., WANG F. Multi-scope electricity-related carbon emissions accounting: A case study of Shanghai. Journal of Cleaner Production. **252**, 119789, **2020**.
26. CHEN H., WANG R.H., LIU X.Y., DU Y.T., YANG Y.T. Monitoring the enterprise carbon emissions using electricity big data: A case study of Beijing. Journal of Cleaner Production. **396**, 136427, **2023**.
27. ZHANG P.F., CAI W.Q., YAO M.T., WANG Z.Y., YANG L.Z., WEI W.D. Urban carbon emissions associated with electricity consumption in Beijing and the driving factors. Applied Energy. **275**, 115425, **2020**.

28. HE Y.Y., WEI Z.X., LIU G.Q., ZHOU P. Spatial network analysis of carbon emissions from the electricity sector in China. Journal of Cleaner Production. **262**, 121193, **2020**.
29. JIANG Z.H., KO D.Y. Decision-making dynamics in urban energy transition: A statistical analysis of policy frameworks, stakeholder collaboration and technological innovations. Sustainable Cities and Society. **109**, 105476, **2024**.
30. PEDDAKAPU K., MOHAMED M.R., SRINIVASARAO P., LICARI J. Optimized controllers for stabilizing the frequency changes in hybrid wind-photovoltaic-wave energy-based maritime microgrid systems. Applied Energy. **361**, 122875, **2024**.
31. YANG W.K., LIU S., WANG Z.Q., LIU H., PAN C.F., LIU C.T., SHEN C.Y. Bioinspired composite fiber aerogel pressure sensor for machine-learning-assisted human activity and gesture recognition. Nano Energy. **127**, 109799, **2024**.
32. GANDOMI A.H., YANG X.S. Chaotic bat algorithm. Journal of Computational Science. **5** (2), 224, **2014**.
33. ZHOU H.M., HUANG G.B., LIN Z.P., WANG H., SOH Y.C. Stacked Extreme Learning Machines. IEEE Transactions on Cybernetics. **45** (9), 2013, **2015**.
34. JIANG N.H., ZHANG J.W., JIANG W.R., REN Y., LIN J., KHOO E., SONG Z.Y. Driving behavior-guided battery health monitoring for electric vehicles using extreme learning machine. Applied Energy. **364**, 123122, **2024**.
35. BOUCHER E., AIRES F. Improving remote sensing of extreme events with machine learning: land surface temperature retrievals from IASI observations. Environmental Research Letters. **18** (2), 024025, **2023**.
36. LI Y., WANG S.L., CHEN L., QI C.S., FERNANDEZ C. Multiple layer kernel extreme learning machine modeling and eugenics genetic sparrow search algorithm for the state of health estimation of lithium-ion batteries. Energy. **282**, 128776, **2023**.